Electronic and Magnetic Properties of K$_2$Mn$_3$S$_4$

G. B. Acharya and M. P. Ghimire

Electronic and Magnetic Properties of K₂Mn₃S₄

G. B. Acharya and M. P. Ghimire*

Central Department of Physics, Tribhuvan University, Kirtipur – 44613, Kathmandu, Nepal
*Corresponding Email: madhav.ghimire@cdp.tu.edu.np

ABSTRACT

Many opto-electronic and energy efficient devices depend on semiconductors' direct as well as indirect band gap. Using spin-polarized density functional theory approach, we calculate the electronic structure and magnetic properties of $K_2Mn_3S_4$. We found that this system has a ferrimagnetic ground state with a saturated magnetic moment of $10\mu_B$ per unit cell. This was mostly caused by the antiferromagnetic interaction between the Mn (I) and Mn (II) atoms, with individual magnetic moment of $4.2 \mu_B$ and $4.1 \mu_B$, respectively. More significantly, from the density of states and band structure calculations, $K_2Mn_3S_4$ is noted as a semiconductor with an indirect band gap of 1.1 eV between the top of the valence band of spin up channel and bottom of the conduction bands of spin down channel, indicating the material as a promising candidate for photovoltaic and opto-electronic devices.

Keywords: Density functional theory, Electronic structure, Semiconductor, Density of states, Magnetic moment.

INTRODUCTION

A semiconductor has an electrical conductivity values that falls between a conductor (say Cu) and an insulator (glass). Si and Ge are two well-known semiconductor elements. Semiconductors have a number of significant properties, including resistivity that is lower than that of an insulator but higher than that of a conductor, a negative temperature coefficient of resistance, the ability to behave as an insulator at absolute zero Kelvin, and the potential to controllably increase conductivity through the semiconductor [1]**.** Well known semiconductors are GaN GaP, GaSb, GaAs, InSb, GaAsSb, AlGaInP, etc. are a few examples [2]. Compound semiconductor offers a significant advantage over element semiconductor in comparison. GaAs, as an example, has the following benefit over Si: (i) A six times increase in electron mobility that enables quicker functioning; (ii) A wider band gap, which enables power devices to operate more faster at higher temperatures and produces less thermal noise at ambient temperatures; (iii) Its optoelectronic properties are more advantageous than those of indirect band gap Si because it has a direct band gap; (iv) For alloying, ternary and quaternary compositions are recommended. In compound semiconductors, nonmagnetic (NM), ferromagnetic (FM), antiferromag-netic (AFM) and ferrimagnetic (FIM) semiconductor are extensively studied theoretically as well as experimentally [3-6]. As a NM semiconductor transistor, bulk inversion asymmetry in (110) InAs/GaSb/AlSb heterostructures was proposed [7]. The magnetic semiconductor research is very attractive, due to its concurrent spontaneous magnetization and semiconducting properties. Furthermore, the doping of magnetic atoms in nonmagnetic materials gives magnetic semiconductors [8-11]. For instance, $SrSn_2Fe_4O_{11}$ is a FM semiconductor having a long range ferromagnetic order, finite remanence, and conductivity that falls exponentially with temperature. Materials with these qualities are intriguing for microwave devices fabrication [12] and also for optoelectronic and photovoltic applications [13, 14]. The FM semiconducting material La_2NiMnO_6 was reported to be very near to room temperature for spintronics applications. The application of a magnetic field can control the magnetic, electrical, and dielectric properties of these magnetic material [15]. Other FM semiconductors which are predicted through the

density functional theory (DFT) is RbLnSe$_2$ (Ln = Ce, Pr, Nd, Gd) [16]. Sr$_2$IrO$_4$ is an AFM semiconductor, reported experimentally having anisotropic magnetoresistance [17]. A ternary selenide Na$_2$Mn$_3$Se$_4$ is an indirect band gap semiconductor with a 1.59 eV gap size that exhibits severely frustrated AFM ordering at 27 K [18]. Though magnetic semiconductors have numerous applications, there are very few materials available. This motivated us to explore several magnetic semiconductor materials**.** The theoretical electronic structure of K$_2$Mn$_3$S$_4$ has not been reported yet. In this study, we used the DFT to analyze the electronic structure and magnetic characteristics of experimentally synthesized K$_2$Mn$_3$S$_4$. Till date, their electronic structure and magnetic properties has not been fully explored. Based on our findings, we predict that the FIM semiconductor K$_2$Mn$_3$S$_4$ can have a net magnetic moment of 10 μ_B per unit cell. This was mainly driven by antiferromagnetic coupling between the Mn (I) and Mn (II) sites. K$_2$Mn$_3$S$_4$ also possesses an indirect band gap of 1.1 eV.

METHODS

To perform the DFT calculation, we used the full-potential local orbital code (FPLO) [19], version 18.00-52, within the generalized gradient approximation (GGA). A localized atomic basis and full potential treatment is applied to analyze the electronic band structure and associated characteristics of K$_2$Mn$_3$S$_4$ using DFT. The exchange-correlation energy functional employed is based on Perdew, Burke, and Ernzerhof's (PBE-96) [20] parameterization. We used the experimentally synthesized material crystal information such as unit cell dimension and atomic Wyckoff positions with full relaxation. A 12 × 12 × 12 k-mesh grid sample is used for the Brillouin zone. The energy and force convergence criteria were set to be 10^{-8} eV and 10^{-3} eV/ Å respectively.

RESULTS AND DISCUSSION
a. Crystal structures

K$_2$Mn$_3$S$_4$ has been reported to be a monoclinic structure with symmetry space group P2/c (space group no. 13). By fusing potassium carbonate and manganese in a stream of hydrogen sulfide at 900 °C, K$_2$Mn$_3$S$_4$ has been synthesized [21]. The structure has three dimensions. There are two inequivalent K^{1+} sites, Mn^{2+} sites and S^{2-} sites denoted by K (I), K (II), Mn (I), Mn (II), S (I) and S

(II) respectively. Eight S^{2-} atoms are connected to both K^{1+} sites via a cubic bond with a body-centered shape. In order to create a mixture of corner and edge-sharing MnS$_4$ tetrahedra, Mn^{2+} is bound to four S^{2-} atoms at both Mn^{2+} sites. S^{2-} is linked to four K^{1+} and three Mn^{2+} atoms in the first S^{2-} site in a 3-coordinate geometry. S^{2-} is linked to four K^{1+} and three Mn^{2+} atoms in the second S^{2-} site in a 7-coordinate geometry as shown in figure 1(a). The respective Brillouin zone (BZ) for the crystal is shown in figure 1(b). K$_2$Mn$_3$S$_4$ has a non-symmorphic symmetry and is a centrosymmetric crystal system. The experimental lattice parameter that we used for our calculations are a = 7.244 Å, b = 5.822 Å, c = 11.018 Å and angles α = 90°, γ = 90° and β =112.33^o [21].
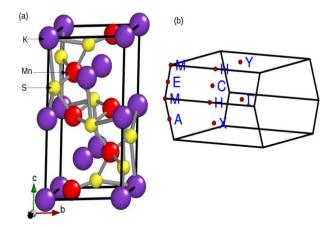

Fig. 1: (a) Crystal structure of K$_2$Mn$_3$S$_4$; (b) 3-D Brillouin zone of K$_2$Mn$_3$S$_4$. The red dot indicates the high symmetry point in the momentum space.

b. Electronic and magnetic properties

We start interpreting our results of K$_2$Mn$_3$S$_4$ by confirming that the material has a FIM ground state. To understand the electronic properties we analyze the total and partial density of states (DOS) within GGA calculation **as** shown in figure 2, wherein the main contributions above the Fermi level (E$_F$) in spin-up channels are from Mn (II)-3d and spin-down channels from Mn (I)-3d orbitals. Below E$_F$, the contributions are from Mn (I)-3d in spin-up channel and in spin-down channel contributions are from Mn (II)-3d states hybridizing with the S-3p states. Exchange coupling between the spin-up and spin-down DOS close to E$_F$ are prominently contributed by Mn (II)-3d with an exchange energy of ~2 eV, while for Mn (I) the exchange energy is found to be approximately 3 eV, respectively.
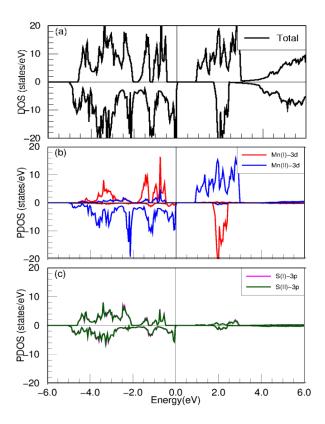
Fig. 2: (a) Total DOS of $K_2Mn_3S_4$ and (b & c) partial DOS for for both inequivalent S and Mn atoms without SOC. The Fermi level is set to zero.
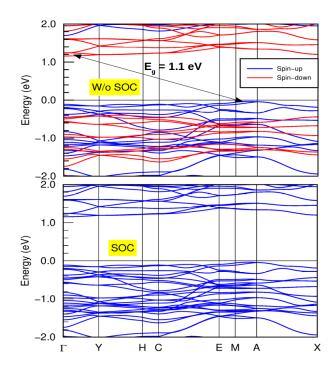

Fig. 3: Electronic band structure of $K_2Mn_3S_4$ in scalar (top) and full-relativistic (bottom). Horizontal solid line indicates the Fermi level. Arrow denotes the indirect band gap between the high symmetry point that lies in the different energy of the momentum space.

The electronic band structure of $K_2Mn_3S_4$ in scalar and full-relativistic (with spin orbit coupling (SOC)) are shown in figure 3. In scalar-relativistic case, the valence band maximum (VBM) lies in MA while the conduction band minimum (CBM) lies at ΓY line in the momentum space resulting in an indirect band gap between VBM and CBM [see figure 3(a)]. $K_2Mn_3S_4$ is thus a semiconductor with an indirect band gap of 1.1 eV.

The effect of SOC is minimal and retains the similar size of band gap within full-relativistic mode. In particular, the band gap value of 1.1 eV which falls in the infrared spectrum is an attractive choice for photovoltaic and optoelectronic devices. From our total energy calculations considering three magnetic configurations: namely FM, AFM, and FIM, the magnetic ground state is found to be FIM. The magnetic easy axis is found to be [001] with hard axis along [010] direction. The computed effective magnetic moments are found to be 10 μ_B per unit cell while the individual moments calculated is 4.2 μ_B for Mn (I), and 4.1 μ_B for Mn (II), respectively. This demonstrates that Mn (I)-Mn (II) couples antiferromagnetically in the ferrimagnetic compound $K_2Mn_3S_4$.

CONCLUSIONS

In conclusion, we perform the density functional theory calculations of K2Mn3S4 which has not been explored so far after the material was synthesized. $K_2Mn_3S_4$ is found to be a semiconductor with an indirect band gap of ~1.1 eV. The ferrimagnetic ground state of $K_2Mn_3S_4$ has a total magnetic moment of 10μ_B per unit cell. This magnetic moment was mostly created by the antiferromagnetic interaction between Mn (I) and Mn (II) atoms. The effect of spin orbit coupling is found negligible. The identification of $K_2Mn_3S_4$ as an indirect band gap magnetic semiconductor is expected to open new door for experimental research that could be used in the fabrication of new devices including semiconductor lasers, solar cells, and light-emitting diodes.

ACKNOWLEDGMENTS

REFERENCES

[1] Braun, D.; Heeger, A. J.; & Kroemer, H. Improved efficiency in semiconducting polymer light-emitting diodes. *Journal of electronic materials*, **20**(11): 945-948 (1991).

[2] Kasap, S. O.; & Capper, P. (Eds.). *Springer handbook of electronic and photonic materials,* New York: Springer, **11**: (2006).

[3] Bhandari, S. R.; Yadav, D. K.; Belbase, B. P.; Zeeshan, M.; Sadhukhan, B.; Rai et al. Electronic, magnetic, optical and thermoelectric properties of Ca$_2$Cr$_{1-x}$Ni$_x$OsO$_6$ double perovskites. *RSC advances*, **10**(27): 16179-16186 (2020).

[4] Bhandari, S. R.; KC, S.; Lawaju, S.; Thapa, R. K.; Kaphle, G. C., & Ghimire, M. P. Electronic structure and estimation of Curie temperature in Ca$_2$BIrO$_6$ (B = Cr, Fe) double perovskites. *Journal of Applied Physics*, **130**(17): 173902 (2021).

[5] Mali, B.; Nair, H. S.; Heitmann, T. W.; Nhalil, H.; Antonio, D. et al. Re-entrant spin reorientation transition and Griffiths-like phase in antiferromagnetic TbFe$_{0.5}$Cr$_{0.5}$O$_3$. *Physical Review B*, **102**(1): 014418 (2020).

[6] Joshi, R. K.; Bhandari, S. R.; & Ghimire, M. P. Structural stability, electronic, optical, and thermo-electric properties of layered perovskite Bi$_2$LaO$_4$I. *RSC advances*, **12**(37), 24156-24162 (2022).

[7] Hall, K. C.; Lau, W. H.; Gündoğdu, K.; Flatté, M. E.; & Boggess, T. F. Nonmagnetic semiconductor spin transistor. *Applied Physics Letters*, **83**(14): 2937-2939 (2003).

[8] Ohno, H. Making nonmagnetic semiconductors ferromagnetic. *Science,* **281**(5379): 951-956 (1998).

[9] Dietl, T. A ten-year perspective on dilute magnetic semiconductors and oxides. *Nature Materials*, **9**(12): 965-974 (2010).

[10] Matthias, B. T.; Bozorth, R. M.; & Van Vleck, J. H. Ferromagnetic interaction in EuO. *Physical Review Letters*, **7**(5): 160 (1961).

[11] Baltzer, P. K.; Lehmann, H. W.; & Robbins, M. Insulating ferromagnetic spinels. *Physical Review Letters*, **15**(11): 493 (1965).

[12] Donchev, V. Surface photovoltage spectroscopy of semiconductor materials for optoelectronic applications. *Materials Research Express*, **6**(10): 103001 (2019).

[13] Mali, B.; Nair, H. S.; Heitmann, T. W.; Nhalil, H.; Antonio, D. et al. Re-entrant spin reorientation transition and Griffiths-like phase in antiferromagnetic TbFe$_{0.5}$Cr$_{0.5}$O$_3$. *Physical Review B*, **102**(1): 014418 (2020).

[14] Shlyk, L.; Strobel, S.; Farmer, B.; De Long, L. E.; & Niewa, R. Coexistence of ferromagnetism and unconventional spin-glass freezing in the site-disordered kagome ferrite SrSn$_2$Fe$_4$O$_{11}$. *Physical Review B*, **97**(5): 054426 (2018).

[15] Rogado, N. S.; Li, J.; Sleight, A. W.; & Subramanian, M. A. Magnetocapacitance and magnetoresistance near room temperature in a ferromagnetic semiconductor: La$_2$NiMnO$_6$. *Advanced Materials*, **17**(18): 2225-2227 (2005).

[16] Azzouz, L.; Halit, M.; Charifi, Z.; Baaziz, H.; Rérat, M.; et al. Magnetic Semiconductor Properties of RbLnSe$_2$ (Ln= Ce, Pr, Nd, Gd): A Density Functional Study. *Journal of Magnetism and Magnetic Materials*, **501**: 166448 (2020).

[17] Fina, I.; Marti, X.; Yi, D.; Liu, J.; Chu, J. H. Anisotropic magnetoresistance in anantiferromagnetic semiconductor. *Nature communications*, **5**(1): 1-7 (2014).

[18] Pak, C.; Garlea, V. O.; Yannello, V.; Cao, H.; Bangura, A. F.; & Shatruk, M. Na$_2$Mn$_3$Se$_4$: strongly frustrated antiferromagnetic semiconductor with complex magnetic structure. *Inorganic Chemistry* (2019).

[19] Koepernik, K.; & Eschrig, H. Full-potential nonorthogonal local-orbital minimum-basis band-structure scheme. *Physical Review B*, **59**(3): 1743 (1999).

[20] Perdew, J. P.; Burke, K.; & Ernzerhof, M. Generalized gradient approximation made simple. *Physical Review Letters*, **77**(18): 3865 (1996).

[21] Bronger, W.; Böhmer, M.; & Schmitz, D. Synthese und Kristallstruktur von K$_2$Mn$_3$S$_4$. *Zeitschrift für anorganische und allgemeine Chemie*, **626**(1): 6-8 (2000).